NATIONAL ADVISORY COMMITTEE FOR AERONAUTICS

TECHNICAL NOTE 4138

CREEP DEFORMATION PATTERNS OF JOINTS UNDER BEARING AND TENSILE LOADS

By E. G. Bodine, R. L. Carlson, and G. K. Manning

Battelle Memorial Institute

Washington

December 1957

NATIONAL ADVISORY COMMITTEE FOR AERONAUTICS

TECHNICAL NOTE 4138

CREEP DEFORMATION PATTERNS OF JOINTS UNDER BEARING AND TENSILE LOADS

By E. G. Bodine, R. L. Carlson, and G. K. Manning

SUMMARY

The objective of the present investigation was to study the interaction of bearing and tensile loads on the creep behavior of joints. To achieve this objective, a simplified model was employed which contained many of the features found in riveted connections. Through the use of this simulated joint, an analysis of complex regions in actual joints could be effected. In the study, results for a number of tensile-to-bearing load ratios were obtained, and the results were analyzed.

It appears that the conclusions listed below can be derived from the findings of this investigation:

(1) The results indicate a reduction in lifetime will occur for a given constant total load as the bearing portion of the load is increased.

(2) From an analysis of the deformations in the area near the simulated rivet hole, it appears that after an initial transient period, a steady-state stress distribution occurs until fracture becomes imminent.

(3) Using conclusion (2) and uniform tensile creep data, stress distributions across the minimum section were computed for the steady-state period. Stress concentrations derived from these results indicated that significant stress relief due to creep had occurred. Strain concentrations, however, continued to increase with time.

(4) It appears that the total deformation of the joint can be partitioned into a plate deformation component (overall plate elongation at the joint) and a hole deformation component (pin movement). The plate deformation component appears to be relatively independent of the loading ratio.[1] The hole deformation component, however, was sensitive to the loading ratio, particularly for high bearing loads.

(5) To achieve a balance of design, it is suggested that the loading ratio in highly stressed regions be kept as high as possible. Relying on stress redistribution as an alternative to balance design may result in excessive joint deformation or premature joint failure.

---

[1]Ratio of total load to bearing load.

INTRODUCTION

The present investigation was conducted at Battelle Memorial Institute under the sponsorship and with the financial assistance of the National Advisory Committee for Aeronautics. It is a continuation of work initiated for the NACA at Battelle in 1954 and reported in reference 1. At that time, it was suggested that further studies be conducted to obtain a more detailed description of the kinematics of deformation of riveted joints subjected to creep. To achieve this objective, the simple joint model developed during the first year's work was subjected to tensile loads, bearing loads, and combinations of tensile and bearing loads. By testing a number of specimens under identical loading conditions but for different lengths of time, it was possible to obtain a detailed analysis of the changing strain pattern. This analysis was then used to establish the manner in which stress redistribution occurs adjacent to the rivet hole. In addition, several other deformation features of the joint model which are characteristic of actual riveted joints have been analyzed and are discussed as a part of the overall objective.

It should be mentioned that although the discussions in the body of the report generally refer to sheet-type riveted connections, the behavior of deformations of the joint-model specimen applies equally well to connections between sheets and heavier sections, such as spars or stringers.

EXPERIMENTAL WORK

Specimens

The specimens used in this study were cut from two 1/8-inch-thick by 4-foot-wide by 8-foot-long sheets of 2024-O aluminum alloy obtained from the same heat. The axis of the specimens was parallel to the direction of rolling. Specimens were 15 inches long and 3 inches wide, with a 9-inch gage section 2 inches wide. A milled hole 0.502 inch in diameter in the center of the gage section served as the simulated rivet hole. (See ref. 1.)

The permanent deformations that occurred during the testing of these specimens were obtained at the completion of the tests from the measurement of a photogrid which was applied to one face of each specimen.

Apparatus

The special fixture shown in figure 1 was constructed for applying both tensile and bearing loads to joint-model specimens at elevated temperatures. Essentially, the apparatus is a lever-type tensile loading frame with an additional lever to apply a bearing load. Since the lines of action of the two forces are superimposed, the bearing load is applied by a pin-and-yolk arrangement so that the bearing load remains independent of the tensile load. Both loads remained constant throughout a test.

The electric furnace which enclosed the specimen maintained the test temperature of 400° F to within 8° F on the 15-inch specimen. Near the central 9-inch reduced section, the temperature variation was less than 4° F. A Minneapolis-Honeywell proportioning controller was used to control the temperature during tests.

Procedure

The elevated-temperature tensile stress-strain diagram (fig. 2) and the tensile creep curves (fig. 3) of the material were obtained from tests performed on standard sheet tensile coupons.

To perform creep tests on the simulated joint specimens, the specimen was placed in the special testing apparatus and a small tensile load was applied. If a bearing load was to be used, a hardened steel pin 0.495 inch in diameter was placed through the hole in the specimen and a small bearing load was applied. The furnace was then closed and the specimen was heated to the test temperature (400° F) in about 40 minutes. After an additional 20-minute temperature-stabilization period, the test load was applied. In the case where the specimen was subjected to both a tensile and bearing load, the two loads were applied together to maintain the proper load ratio.

After a selected interval, the load was removed and the specimen was allowed to cool to room temperature. Measurements were then made of the deformed photogrid. A separate specimen was used for each interval so that a record of the permanent deformations was retained.

Measurement of Strain

The photogrid that was applied to the specimen formed squares measuring 0.050 ± 0.0001 inch and oriented with their sides perpendicular and parallel to the axis of the specimen. After testing, these squares had deformed plastically and their new dimensions were measured. Thus, longitudinal and transverse strains could be obtained.

Measurements were made with a Gaertner micrometer comparator, the smallest reading of which was 0.00005 inch. This implies a sensitivity of 50 microinches. The deviation from the average in four readings for large values of strain (over 10 percent) was never greater than 0.00025 inch, indicating a reproducibility of better than 0.5 percent. Down to about 1-percent strain, the reproducibility was better than 1.0 percent. Corresponding computed strain values were estimated to be accurate to within 7 and 14 percent, respectively.

Application of Photogrid

All joint-model specimens were chemically polished prior to the application of the photogrid. The polishing treatment which was used consisted of agitating the specimen in a hot (190° F) chemical polishing solution composed, by weight, of 1 part of Kaynide Alchemize Bright Dip Concentrate to 9 parts of phosphoric acid (85 percent) for from 2 to 3 minutes, then dipping it in concentrated nitric acid for from 5 to 10 seconds, and then washing it in water. This treatment produced a bright surface suitable for receiving the photogrid emulsion.

After being polished, the specimen was placed in a warmed box (about 140° F) and sprayed with a photographic emulsion of the following composition: 4 parts photoengraver's glue, 23 parts water, 1 part ammonium dichromate, and 1/4 part ammonia water. For spraying, the above solution was diluted by mixing 1 part of the solution to 3 parts of water and 4 parts of ethyl alcohol. Although it was not necessary to perform this work under darkroom conditions, direct exposure to sunlight was avoided. Six thin coats of the diluted emulsion were applied, and a drying time of approximately 20 minutes between applications was allowed.

Negatives made from a diamond-ruled glass plate (20 lines to the inch) were placed over the emulsified face of the specimen, and printing was accomplished by exposure to four No. 2 photoflood lamps. The time for exposure was about 16 minutes, and the distance from bulb to plate was about 1 foot. An electric fan kept the specimen cool during exposure. The printed emulsion was developed by washing the specimen in a solution of clothes dye and water for about 5 minutes. After drying, the grid formed on the specimen was generally impervious to moderate handling and was capable of withstanding exposure to the test temperature of 400° F.

DISCUSSION OF RESULTS

The specimen which was used as a joint model allowed the application of both bearing (through a pin) and tensile loads. A limitation of the model is, however, that rivet-head pressures and subsequent sheet friction cannot be represented.

The method of strain measurement that was used necessitated producing relatively large plastic strains in the test models. These strains, in turn, probably produce residual stresses in the cooled, unloaded specimens. The effect of residual stresses was not assessed, but it is felt that the associated strains were small compared with the large plastic strains.

Static and creep properties for the test material are shown in figures 2 and 3. Figure 4, showing the secondary creep rate as a function of stress, was obtained from figure 3. The creep curve shown for 13,000 psi has been estimated by the use of an isochronous stress-strain curve. It is, therefore, an interpolated curve.

An important factor that has not been investigated in this study is the effect of the geometry of the test model. It is expected that the ratio of hole diameter to width, ratio of hole diameter to thickness, and hole width-to-thickness ratio will have effects on the deformation patterns.

Creep-Rupture Tests

It has been reported that the interaction of tensile and bearing loads on the creep of riveted joints is not expected to affect their time to rupture (ref. 2). The results of creep-rupture tests conducted during the present program agree only in part with this conclusion.

Figure 5 shows the time to failure for a number of simulated joints as a function of the average stress for several values of loading ratio P_t/P_b. (The average stress is defined here as the total load divided by the minimum cross-sectional area; the term "loading ratio" means the ratio of the total load applied to the specimen P_t to the bearing load P_b.) Thus, for a tensile load alone, for example, the ratio would be ∞. The times to failure tend to be ordered with respect to the loading ratio and tend to decrease with increasing bearing load (decreasing values of P_t/P_b). If the variation in stress which occurs at the different loading ratios for a constant time to failure is considered, it can be concluded that the interaction effect is small.

However, if the variation in time to failure for a constant stress is considered, a much more significant difference is seen to exist.

It should be noted that specimens tested at $P_t/P_b = 1$ failed by a local buckling of the plate ahead of the bearing pin instead of by fracture across the minimum section. If the plate were constrained by other plates or by rivet-head pressure, longer times to failure might be expected.

A conclusion which may be reached on the basis of these tests is that an increase in the portion of bearing load carried by a rivet will tend to increase its rate of joint distortion and decrease its useful life.

Plate Subjected to Tension

The problem of the plate with a hole subjected to tension constitutes the limiting case in joint analysis of the rivet which exerts a small bearing force but is situated in an area subjected to a large tensile stress.

Typical permanent longitudinal strains which occur in the simulated joint specimens after a selected time under load are illustrated in figure 6. The variation of these strains across the minimum section A-A is illustrated in figure 7 for one of the test conditions. The stress distribution which corresponds to the initial strains (zero time) is shown in figure 8, and it was obtained from the stress-strain curve by assuming that the stress system is uniaxial. (Within the minimum sections, stresses are actually biaxial. The transverse stresses, however, are small compared with the longitudinal stresses.) The line of average stress is also indicated in the same figure.

Figure 9 shows the strains at selected points on A-A as a function of time. The general appearance of these curves is similar to that of uniaxial creep curves. That is, they appear to exhibit an approximately constant creep rate during part of the test. This constant rate has been taken to imply a fixed or steady-state stress distribution during this period (i.e., the stress on each fiber along A-A is constant during this period). Using the creep rates indicated in figure 9 and the relationship indicated by figure 4, a steady-state stress distribution has been plotted in figure 10. Although the average stress indicated does not correspond exactly to the actual average stress, the agreement is fair.

Several interesting features are evident from a study of figures 5 to 10. The distribution of stresses along line A-A can be expected to change from that of figure 8 to that of figure 10 during an initial adjustment period. Then a period of relatively constant stress distribution occurs, after which the creep rates increase and fracture ensues. During the stage prior to fracture, those fibers nearest the hole, having lost most of their capacity to resist deformation, have elongated sufficiently to cause a further shifting of the load to areas farther from the hole. This shifting of load is evidenced by a general increase in strain rate all across the section.

Since strain rates decrease going away from the hole, lines originally parallel to A-A would be expected to rotate with respect to A-A. (This rotation is easily discerned in the deformed grid.) Finally, fracture initiates at the hole and progresses outward to the edges of the specimen.

Although the elastic stress concentration caused by the presence of the hole is greatly reduced by the plastic deformation associated with the initial loading and is further reduced by creep, it should be mentioned that the strain concentration apparently does not decrease. In addition, the differences in rate of creep elongation for even slight differences in stress (see fig. 4) are evidently so great that strain relief[2] near the edge of the hole does not occur before the ductility of the material at that point is exhausted. Further discussion of stress and strain concentration factors is included in a later section of the report.

The net effect of the strains in the area surrounding the hole is to produce an elongation of both the hole and the plate in the direction of the applied load. Figures 11 and 12 show these elongations after 0 hour, 1/2 hour, and 5 hours under load. The quantities "elongation of the hole" and "elongation of the plate" refer to the percent increase of the hole diameter and the percent increase of the central 4-inch section of the specimen, respectively.

The initial (0-hour) hole elongation resulted mainly from a well-defined plastic zone adjacent to each side of the hole at the points of maximum stress. As the stress level increased, these zones spread symmetrically at 45° to the axis forming a large letter "X" concentric with the hole, as illustrated in figure 6.

As would be expected, it was possible to predict the magnitude of hole elongation from the strain pattern adjacent to the hole. In addition, it was also possible to estimate the plate elongation from the magnitude of the strains near the outer edge of the specimen. The

---

[2]A decrease in the ratio of the total strain adjacent to the hole to that away from the hole. It should be remembered that both of these strain values continued to increase with time.

latter calculation was simplified by the fact that, for a given time not near fracture, the edge strains are relatively constant along a large section of the specimen (see fig. 6).

In order to obtain an estimate of the hole elongation, a slightly more elaborate calculation was necessary. The strains along the axially directed line immediately adjacent to the hole were integrated to yield the increase in length of the segment of the line which corresponded to the original diameter of the hole. It was then assumed that the rotation of lines originally parallel to line A-A (fig. 6) occurred without any curving of the lines.[3] Therefore, considering the geometry of the specimens, the increase in the diameter of the hole would be 1.33 times the increase in the length of the adjacent line. (The slight contribution of the outer edge strains has been neglected.) Actually, a better estimate was obtained if the factor used was about 1.6, indicating that curving of the lines does occur near the hole.

Plate Subjected to Bearing Loads

The plate with a hole subjected to bearing loads ($P_t/P_b = 1$) simulates the condition existing at the end rivets in, for example, the simple lap joint. It should be noted that studies have been conducted on both the plastic deformations (ref. 3) and the creep deformations (ref. 4) which occur in bearing. For the most part, these studies were confined to "overall" deformations and they did not evaluate local strain distributions.

The permanent axial strains which resulted from the application of a bearing load for a specified time are typified by figure 13. The permanent strains for the corresponding specimen subjected to tension alone are included in the same figure. It can be seen that the strains near the hole on line A-A are much larger for the case of bearing than for that of tension, even though the average stress across A-A is the same in both cases. At the outer edge of the specimen, however, the strains are nearly equal. Further observation of the deformations for the specimen of figure 13 suggests that the stress system was as shown in figure 14. (Only the longitudinal stresses are shown.) It can be seen from figure 14 that a limited section near the outer edge of the specimen behaves as though it were loaded in tension. However, the rapid transition from compression to tension along the axially directed line adjacent to the hole does not have a counterpart in the specimen subjected to tension alone. The strains resulting from this type of loading indicate that the rate of creep deformation in the area of the hole is faster for the case of bearing. Also, if the bearing load is

---

[3] A visual inspection of the deformed grid lines indicated that this was a fair assumption.

large enough, the rate of elongation of the plate will be greater than that for the equivalent tensile load $\left(P_t/P_b = \infty\right)$. For small bearing loads, however, the presence of the bearing does not appear to influence the elongation of the plate greatly.

As for the case of the plate subjected to tension, the hole elongation, plate elongation, and stress concentration factors have been obtained for the plate in bearing and will be included in the following section.

Plate Subjected to Tensile and Bearing Loads

In addition to the investigation of the plate subjected to tension and the plate subjected to bearing, two conditions of combined loading were studied. For the first, the bearing and tensile loads were equal $(P_t/P_b = 2)$ and for the second the tensile load was twice as great as the bearing load $(P_t/P_b = 3)$.

The permanent longitudinal strains that occurred in a typical specimen subjected to combined loading are shown in figure 15. In the same figure are the strains for the corresponding specimen subjected to tension alone. As was the case for the plate subjected to bearing, the strains near the hole are greater for the combined loading than for tension alone. They were not, however, as large as those produced by the same load applied in bearing alone. This is also evidenced by the fact that the corresponding specimen subjected to bearing alone failed prior to the scheduled removal of the load.

As before, stresses were calculated on the basis of strains and strain rates. The stress and strain concentration factors are given in table 1 for all four conditions of initial loading (zero time). (Stress and strain concentration factors were based on a comparison of the maximum stresses and strains adjacent to the hole with those far below the hole.) The stress concentration factors given in table 2 are for the distribution during the constant-creep-rate period. Strain concentration factors were not obtained after the initial loading.

The values of these concentration factors indicate that the stress relief that occurs due to the initial plastic deformations varies with the applied load and is greater for high loads. It should be mentioned that although stress concentration factors become smaller the maximum stress does not decrease as the load is applied. As creep takes place, a still further reduction in concentration occurs and the limiting value of stress concentration is approached for all loading conditions. (This limiting value is given by the ratio of the area of the specimen away from the hole to that including the hole, and is 1.33.) The strain concentrations, however, do not approach a finite limit and apparently continue to increase both with load and with time until fracture occurs.

The data given in tables 1 and 2 suggest that the selection of materials used for joints should be based, for the most part, on available ductility. For example, a material which has high strength but relatively low ductility does not take full advantage of the stress relief which is coincident with plastic flow. On the other hand, a material of moderate strength which has the ability to withstand large deformations more fully utilizes its maximum strength and may prove more useful as a joint.

Figures 16 and 17 summarize the data for plate and hole elongations for the four loading conditions studied. These plots isolate the two sources of joint deformation - elongation of the plate adjacent to the hole and pin movement (hole elongation).

In the use of a joint exposed to bearing and tensile loads, it would be of interest to know the extent of the region over which the deformation behavior is influenced by the presence of the hole. To obtain an idea of the size of this region, an attempt was made to compute an effective length in which all of the deformation could be considered to occur. Well above and below the minimum section, the strains were, comparatively, quite small. An effective gage length, l can be estimated as

$$l = \frac{\Delta}{\epsilon}$$

where Δ is the rate of increase in the length of the plate containing the hole and ϵ is the average strain rate along the outer edge of the plate near the minimum section.

As indicated above, the deformation rate distant from the minimum section is small. An estimate of Δ can, therefore, be obtained by multiplying the elongation rates of figure 16 by 4 inches (the gage length for these curves). Since ϵ can be obtained from the experimental data, it is possible to compute values of l for the various loading ratios. The result of these computations is given in table 3. The values in table 3 indicate that, for the joint studied, the region of plate influenced by the presence of the hole was approximately 1.3 inches (2.6 hole diameters).

The initial (zero-time) elongations of the bearing hole were not too evident from figure 17, so figure 18 was prepared. Figure 18 shows the elongation of the hole due to bearing alone and was obtained by assuming that the hole elongations were made up of an elongation due to bearing and an elongation due to tension. The elongation due to bearing alone would then be the hole elongation minus the elongation due to tension. The straight line of the figure shows the trend of the plotted points and indicates that the hole elongation due to bearing is a linear function of the bearing load. During creep, however, the rate of hole elongation due to bearing (total rate minus tensile rate) varies with the bearing load in the manner shown in figure 19 and illustrates the tendency of large bearing loads to increase abruptly the rate of deformation near the hole.

Index of Joint Behavior

In order to be able to discover the effect of combined loading on an actual joint, it was desirable to obtain an index of joint behavior from the simulated joints that were tested during this investigation. This index was obtained from a consideration of the total elongation in a simple one-rivet lap joint. For this case, the total elongation which would occur in a specified gage length would be the sum of the plate extension and the rivet-hole elongation for each of the two plates. In other words, if E_p was the individual plate elongation and E_h was the individual hole elongation, the total elongation would be

$$T = \frac{E_p}{2} + E_h + E_h + \frac{E_p}{2}$$

or

$$T = E_p + 2E_h$$

The value of $E_p + 2E_h$ has been taken to be the desired index of joint behavior.

Values of E_p, E_h, and T can be obtained from figures 16 and 17 for a joint of the same dimensions as the simulated joint specimens. This has been done to obtain figure 20. Figure 20 shows the total elongation T (over 4 inches) as a function of loading ratio. (It is recognized that the abscissa values other than 1/1 cannot exist for a simple single riveted lap joint. For the remaining values of the index, however, the plot serves to indicate that the load carrying capacity of a sheet can be markedly improved by increasing the loading ratio.) It can be seen from figure 20 that resistance to deformation increases with increasing loading ratio (P_t/P_b) and decreasing stress. These results suggest that as the bearing component of the load becomes large, the deformation at a connection increases rapidly. This is particularly true as time increases.

REMARKS ON DESIGN OF JOINTS SUBJECTED TO CREEP

From the discussion of creep-rupture tests and of the plate subjected to tension and bearing it can be concluded that, to produce the least deformation in a riveted joint, the loading ratio at critical sections of the joint (areas of highest stress) should be kept as large as possible. A corollary of this conclusion is that the bearing load at rivets subjecting the plate to pure bearing should be placed at areas of minimum stress. The application to design of these two principles can be best illustrated by several possible joint designs.

A simple lap joint having three rows of rivets is shown in figure 21(a). If only the upper plate is considered, at the critical area (line A) the initial loading ratio is 3. It would be expected that this joint would deform most rapidly (and eventually fail) along line A. If the thickness of the plates forming the joints were tapered slightly, as in figure 21(b), to produce less bearing in the end rivets, the loading ratio at the critical area could be increased.

The same effect could be obtained more practically by increasing the number of rivets along line B as shown in figure 21(c). With this modification there will be an improved deformation distribution near A at the expense of that near B. The average stress at B, however, is significantly lower than that at A so that an overall improvement in the joint behavior could be expected.

It is recognized that during the course of initial loading and during subsequent creep deformation a redistribution of loading will occur within a joint or connection that will tend to alleviate the situation in highly stressed areas. It may, hence, be felt that the value of the loading ratio is not too significant after all. It should be remembered, however, that this may occur at the expense of significant joint deformation. Also, if local deformation in a particular region is permitted to become excessive, the material damage incurred may materially reduce the life of the joint. An initially balanced design, therefore, appears to be essential.

Battelle Memorial Institute,
Columbus, Ohio, July 9, 1956.

REFERENCES

1. Bodine, E. G., Carlson, R. L., and Manning G. K.: Interaction of Bearing and Tensile Loads on Creep Properties of Joints. NACA TN 3758, 1956.

2. Mordfin, Leonard, and Legate, Alvin C.: The Creep Behavior of Structural Joints of Aircraft Materials Under Constant Loads and Temperatures. Rep. 4052, Project S55-50, NACA and Nat. Bur. Standards, Apr. 20, 1955.

3. Anon.: Strength and Testing of Materials. Pt. II. Selected Govt. Res. Reps., vol. 6, Dept. Sci. and Ind. Res., Ministry of Supply, 1952.

4. Vawter, F. J., Guarnieri, G. J., Yerkovich, L. A., and Derrick, G.: Investigation of the Compressive, Bearing and Shear Creep-Rupture Properties of Aircraft Structural Metals and Joints at Elevated Temperatures. TR 54-270, pt. 1, Contract No. AF 33(616)-190, WADC and Cornell Aero. Lab., Inc., June 1954.

TABLE 1.- STRESS AND STRAIN CONCENTRATION FACTORS

FOR INITIAL LOADING

Average stress, psi	Load ratio of -			
	∞	3	2	1
	Stress concentration factors			
13,230	1.55	-----	-----	-----
11,200	1.53	1.72	-----	-----
10,240	1.58	1.58	1.64	1.54
9,390	1.62	1.68	1.68	1.55
	Strain concentration factors			
13,230	11.4	-----	-----	-----
11,200	9.4	16.5	-----	-----
10,240	7.9	7.9	10.4	6.5
9,390	5.6	6.9	6.9	4.4

TABLE 2.- STRESS CONCENTRATION FACTORS DURING CREEP

Average stress, psi	Stress concentration factors for load ratio of -			
	∞	3	2	1
13,230	1.43	----	----	----
11,200	1.44	1.43	----	----
10,240	1.45	1.41	1.47	1.49
9,390	1.45	1.48	1.41	1.64

TABLE 3.- EFFECTIVE GAGE LENGTH FOR

LOADING RATIOS TESTED

Load ratio, P_t/P_b	Effective gage length, in., for average stress, psi, of -			
	13,230	11,200	10,240	9,390
∞	[a]1.84	1.32	1.32	1.32
3	----	1.32	1.24	.92
2	----	----	1.16	1.32
1	----	----	1.48	1.00

[a]Fracture imminent.

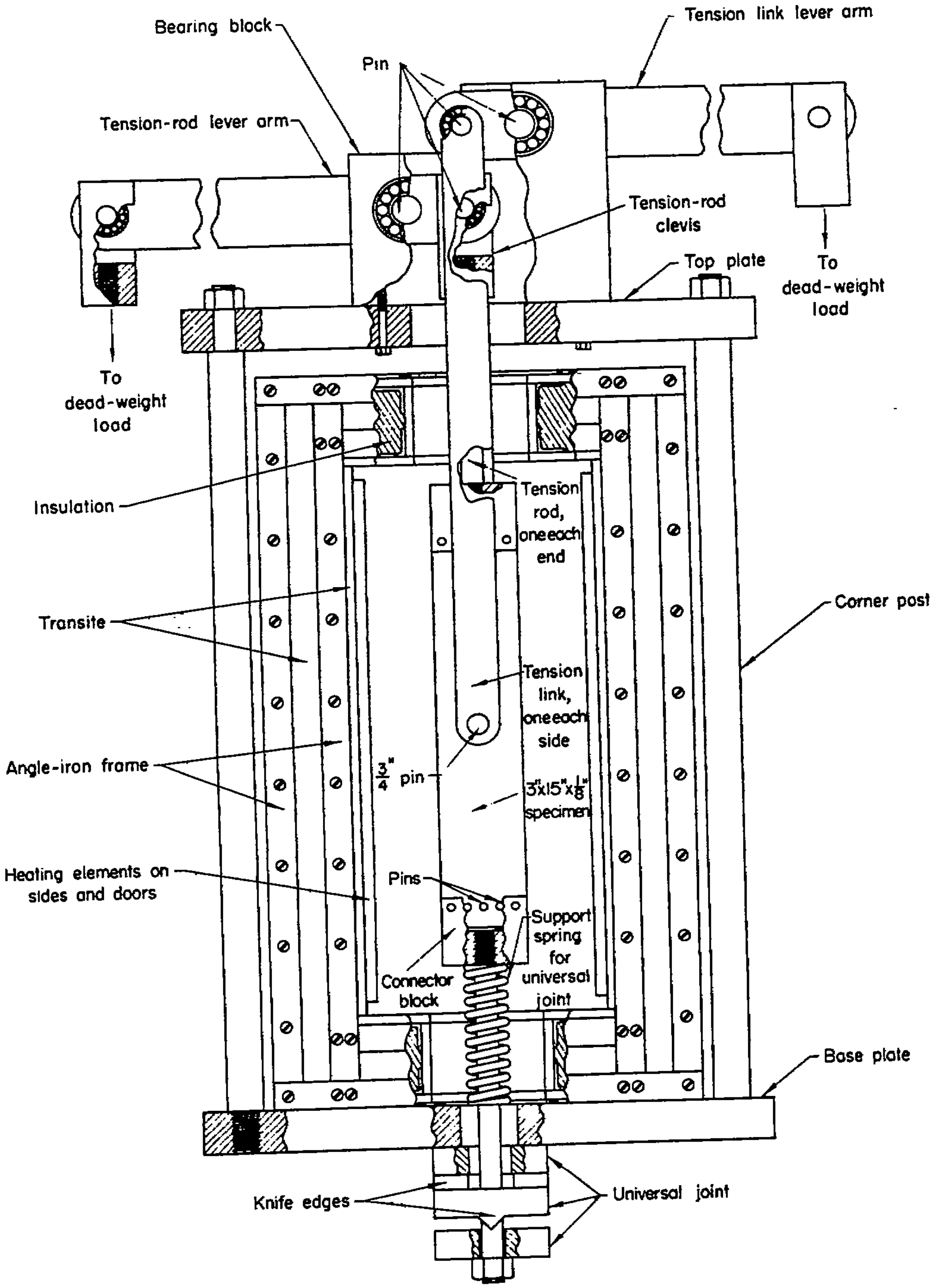

Figure 1.- Loading-frame unit. Furnace shown looking into access doorway; door removed.

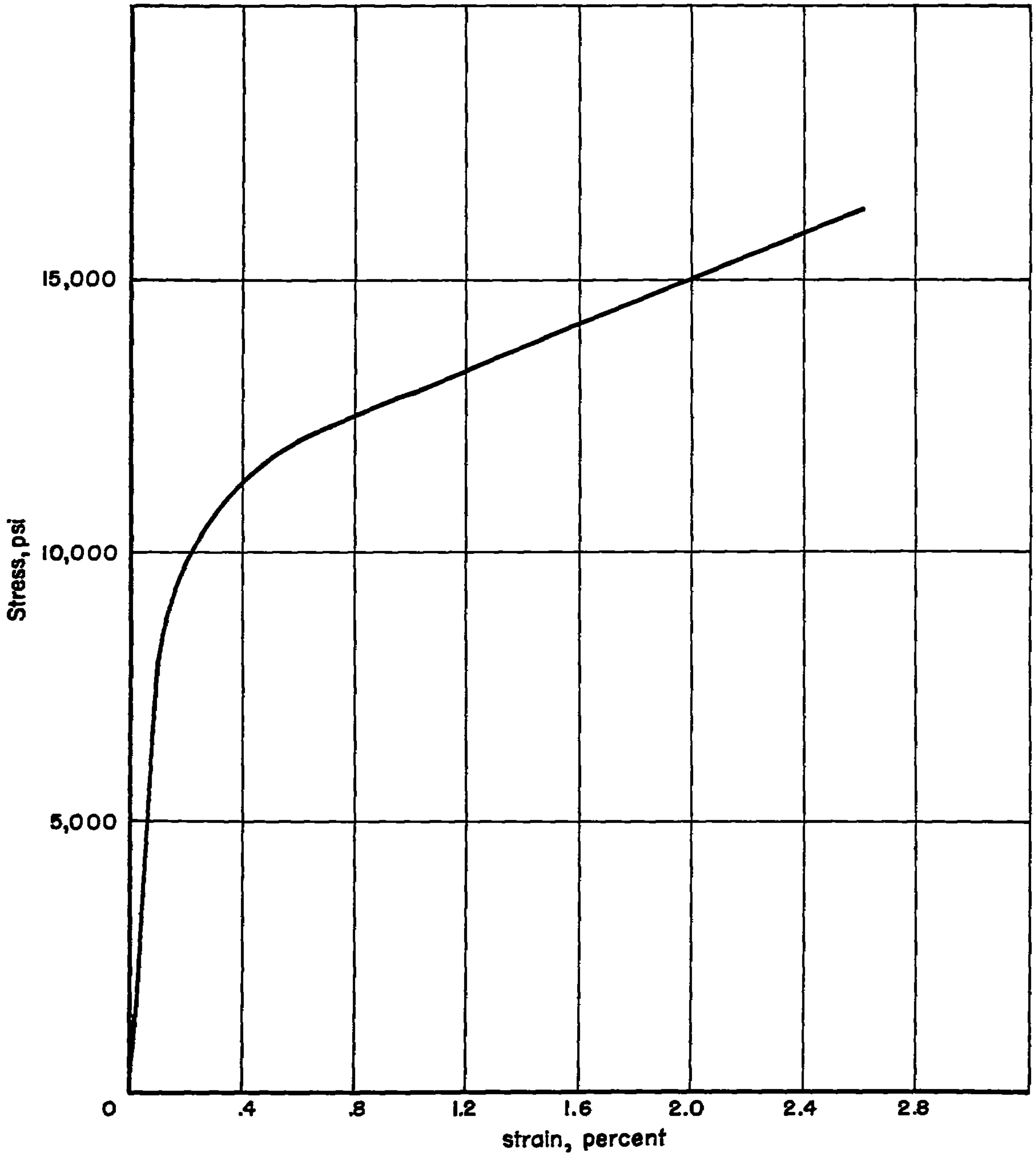

Figure 2.- Stress-strain diagram of 2024-0 aluminum alloy tested in tension at 400° F. Curve is average of results for three tests.

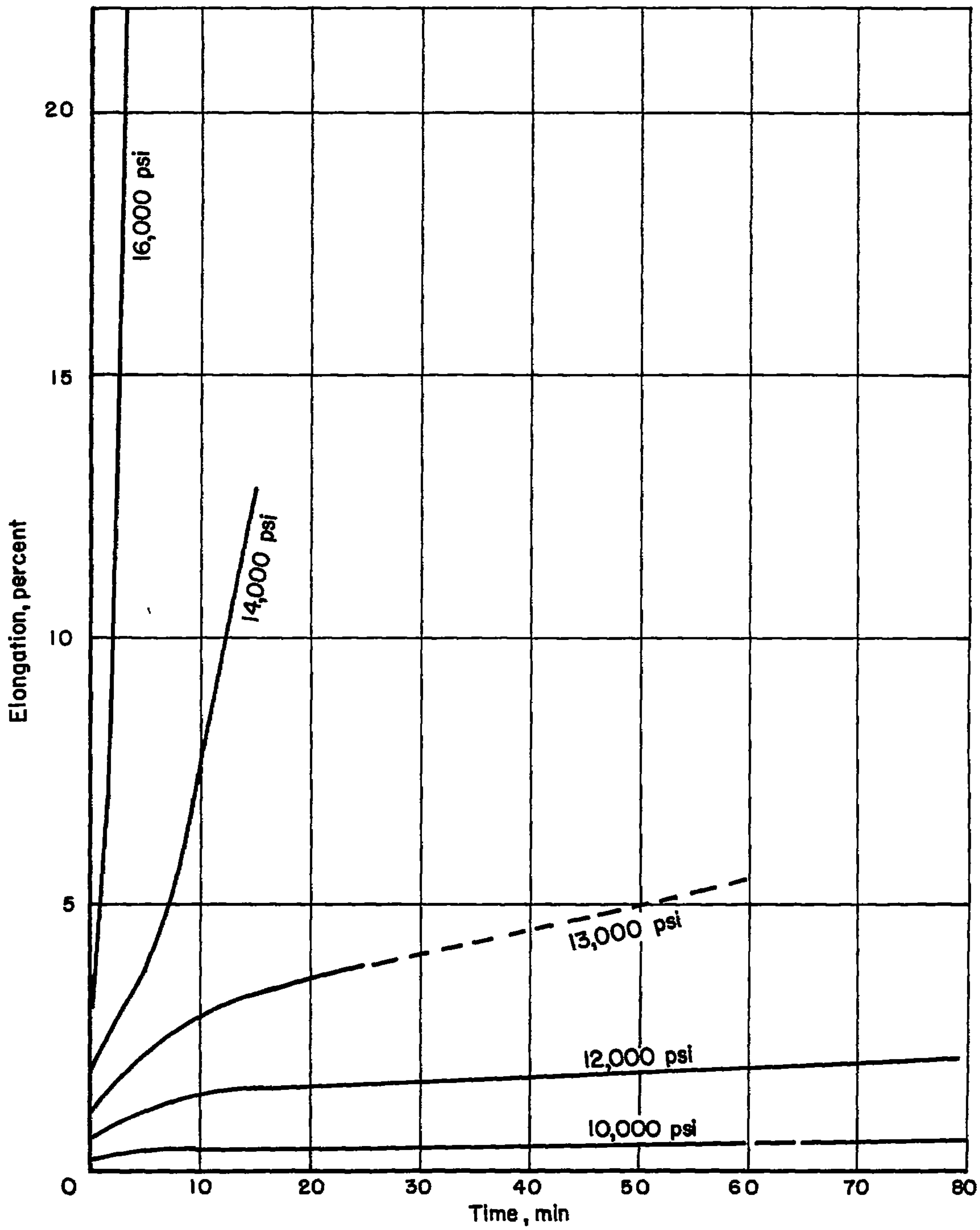

Figure 3.- Tensile creep curves for 2024-0 aluminum alloy tested at 400° F.

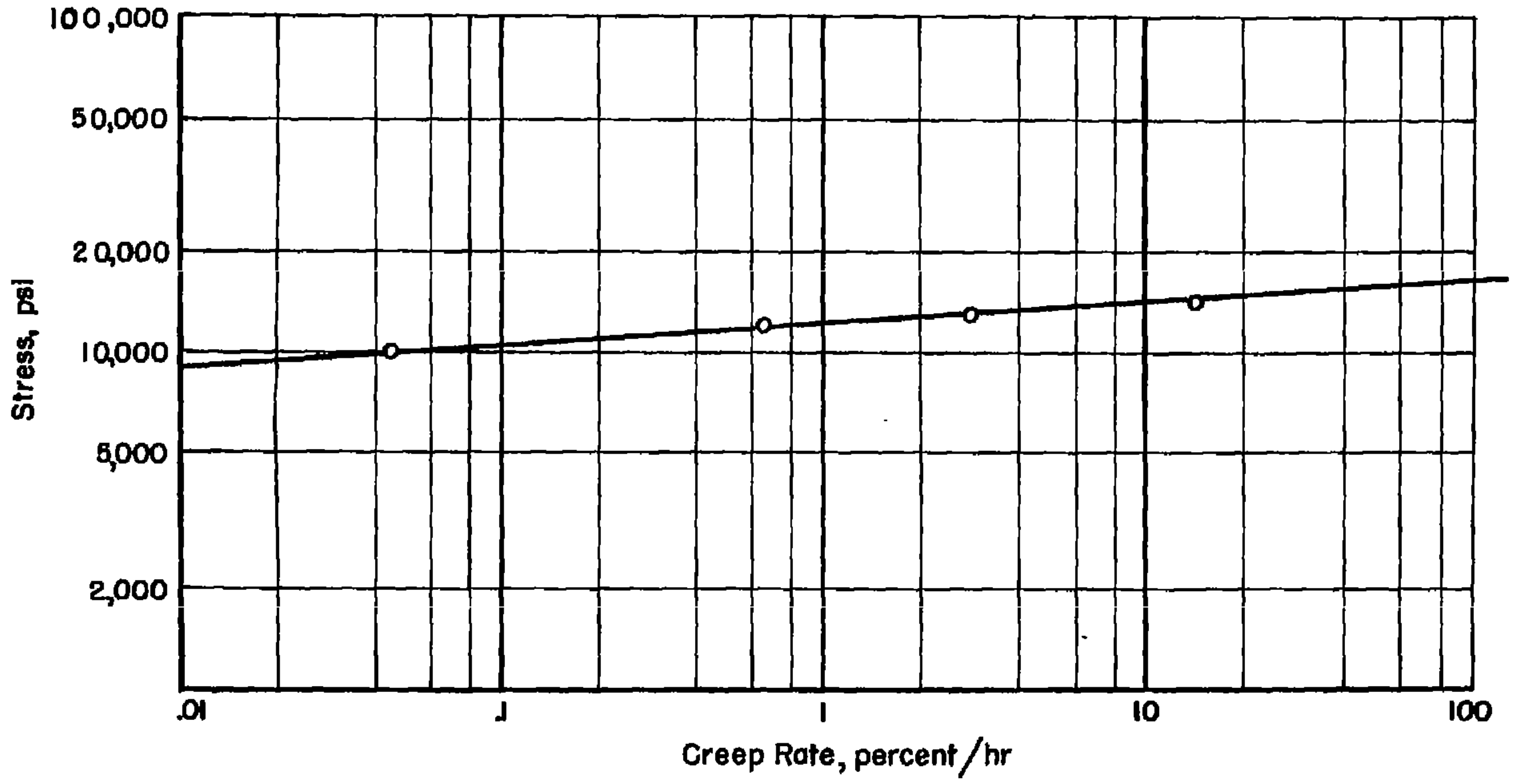

Figure 4.- Secondary creep rate as a function of stress for 2024-0 aluminum alloy tested in tension at 400° F.

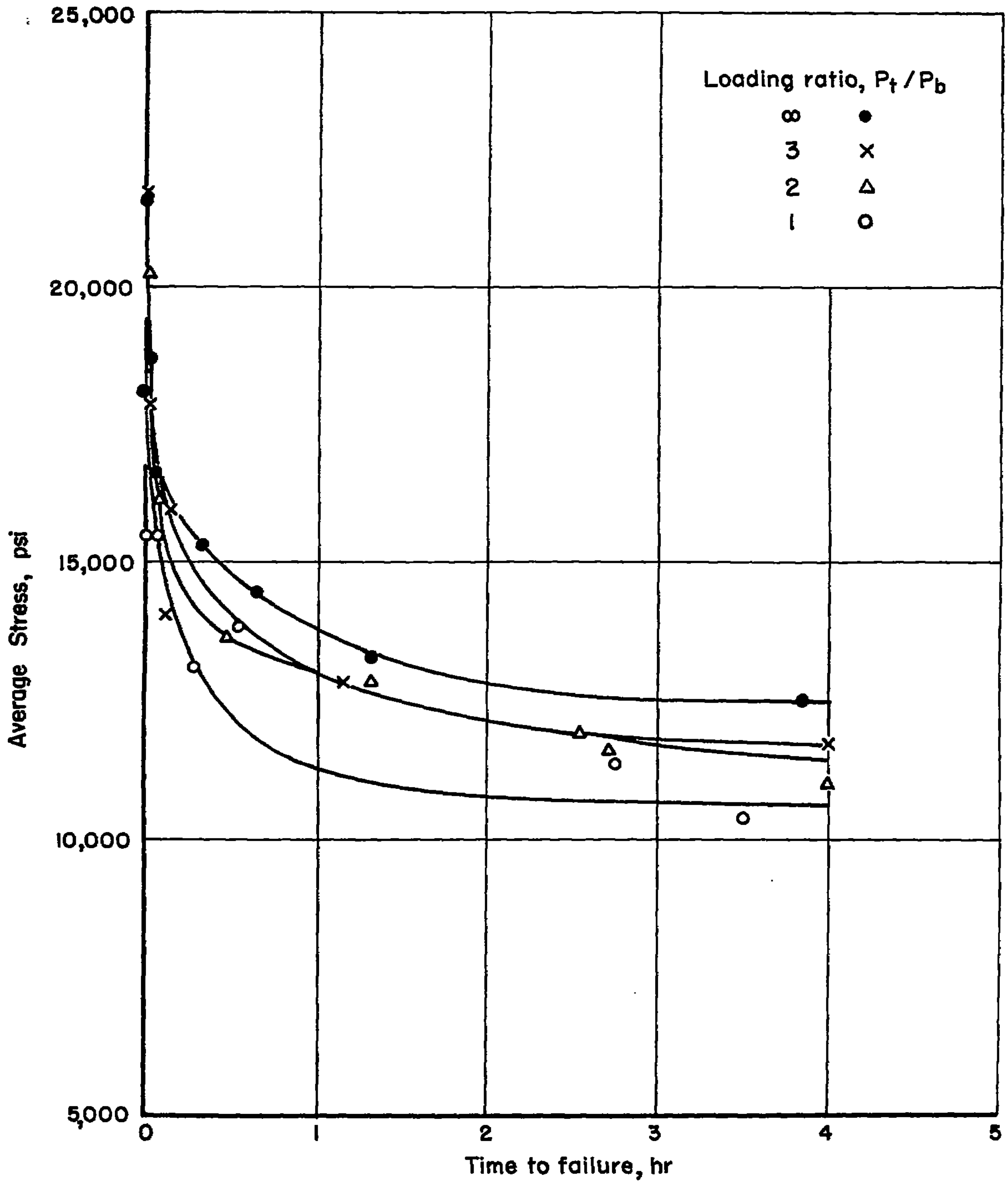

Figure 5.- Creep-rupture curves for simulated riveted joints subjected to four loading conditions. Test temperature, 400° F.

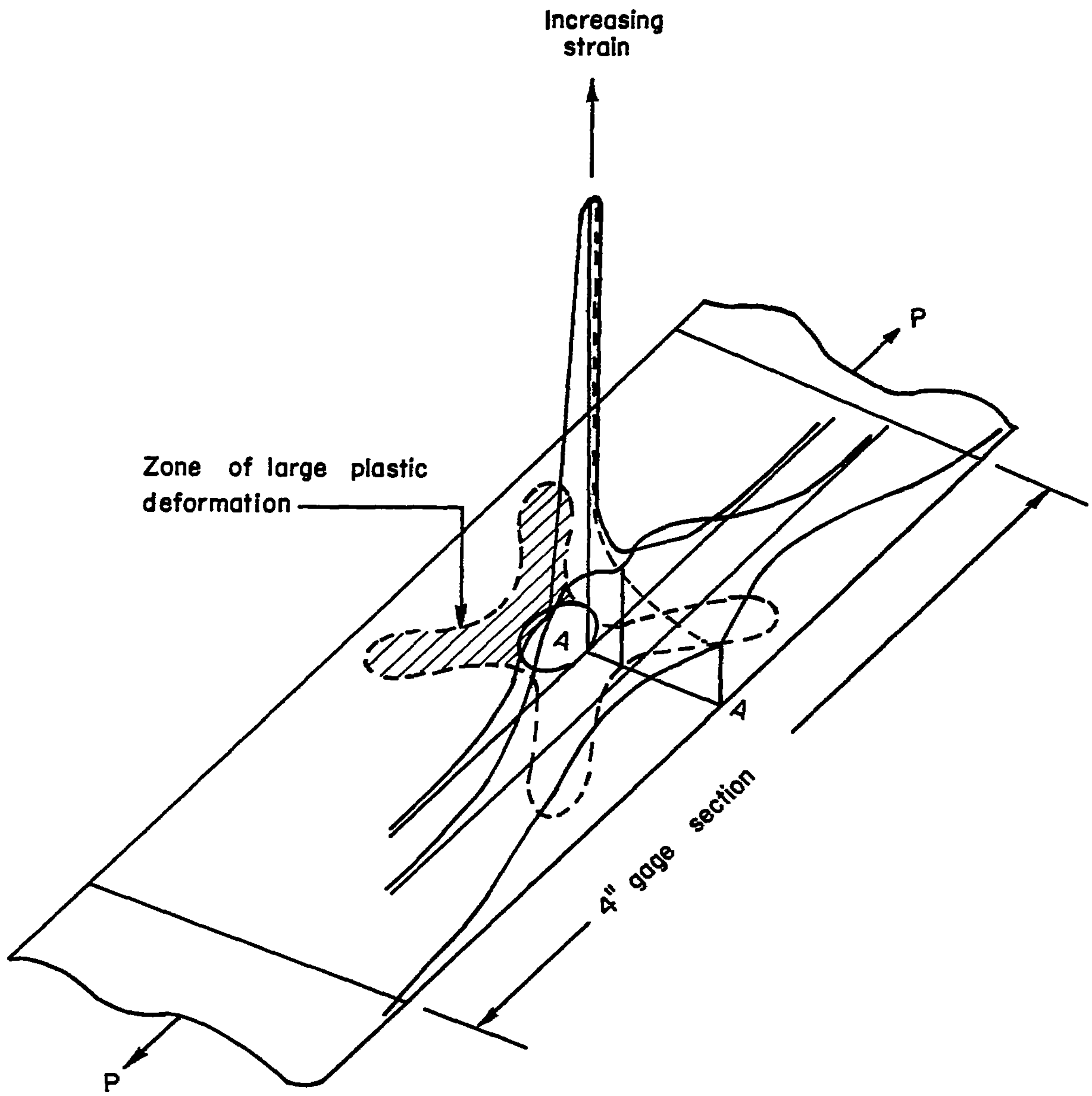

Figure 6.- Typical longitudinal strains in plate with a hole subjected to tension.

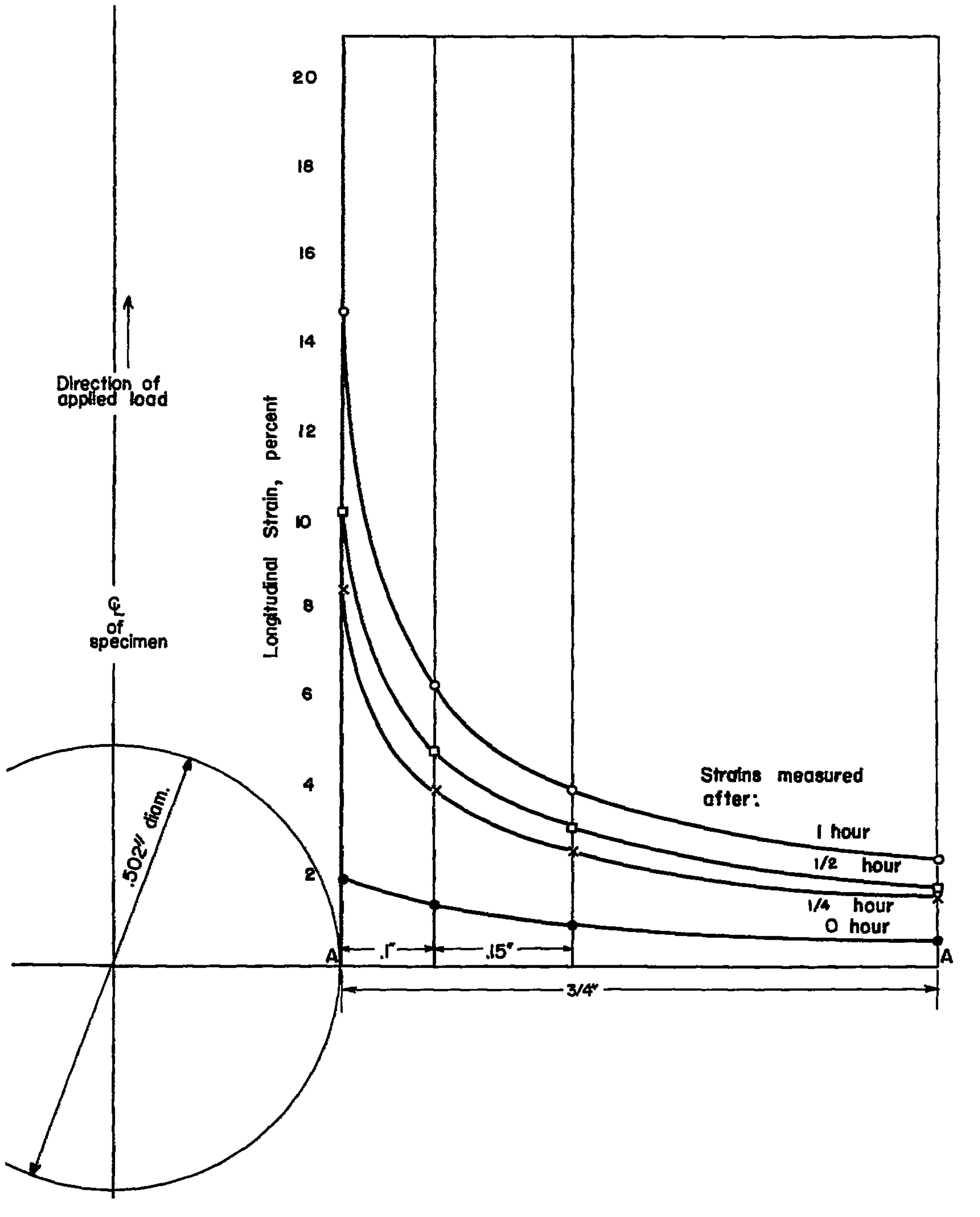

Figure 7.- Permanent strains on line A-A in plate subjected to tension. Test temperature, 400° F; load, 2,480 pounds; average stress across A-A, 13,230 psi; loading ratio P_t/P_b, ∞.

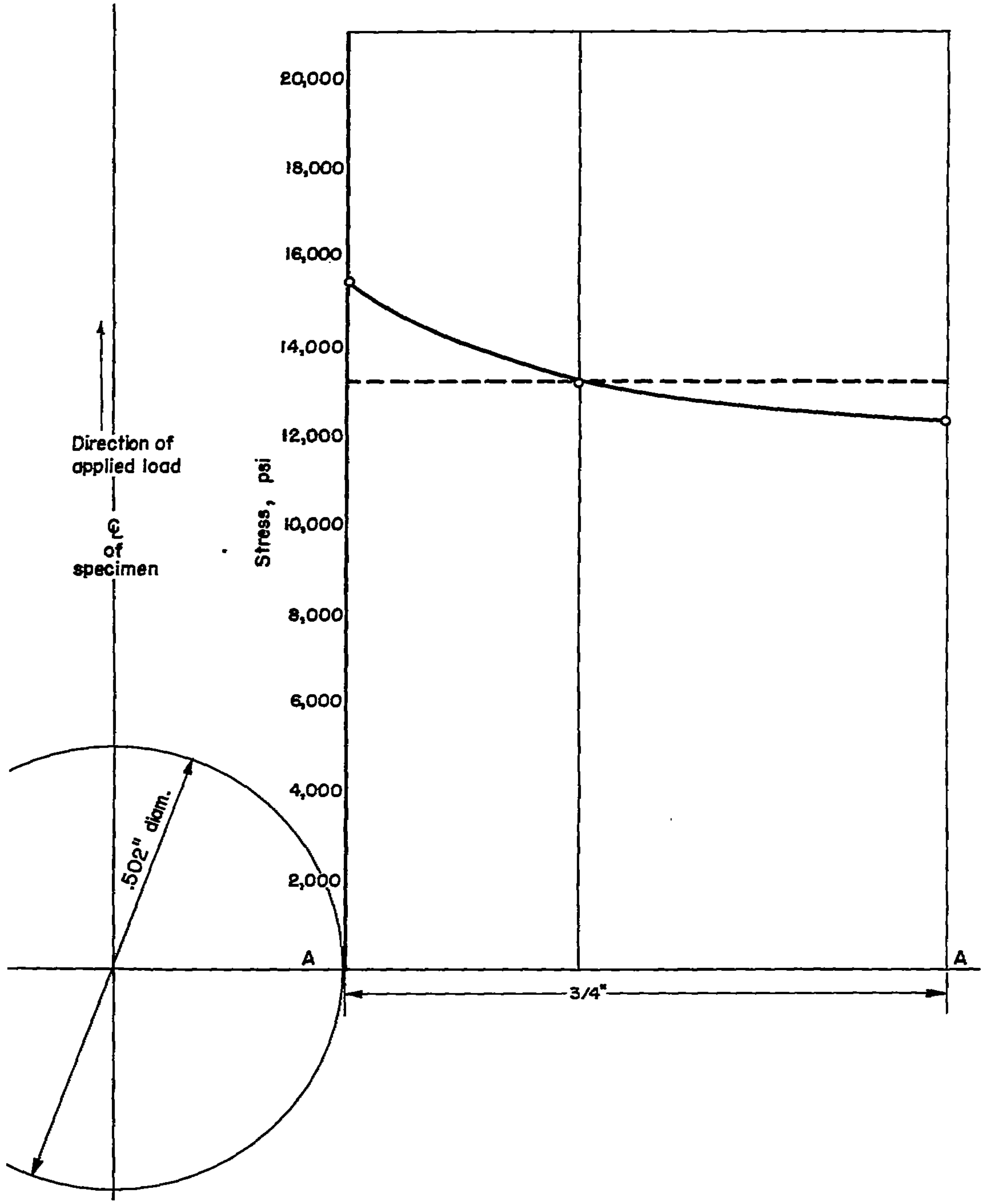

Figure 8.- Initial stress distribution (0 hour) on line A-A in plate subjected to tension. Broken curve denotes average stress. Test temperature, 400° F; load, 2,480 pounds; loading ratio P_t/P_b, ∞.

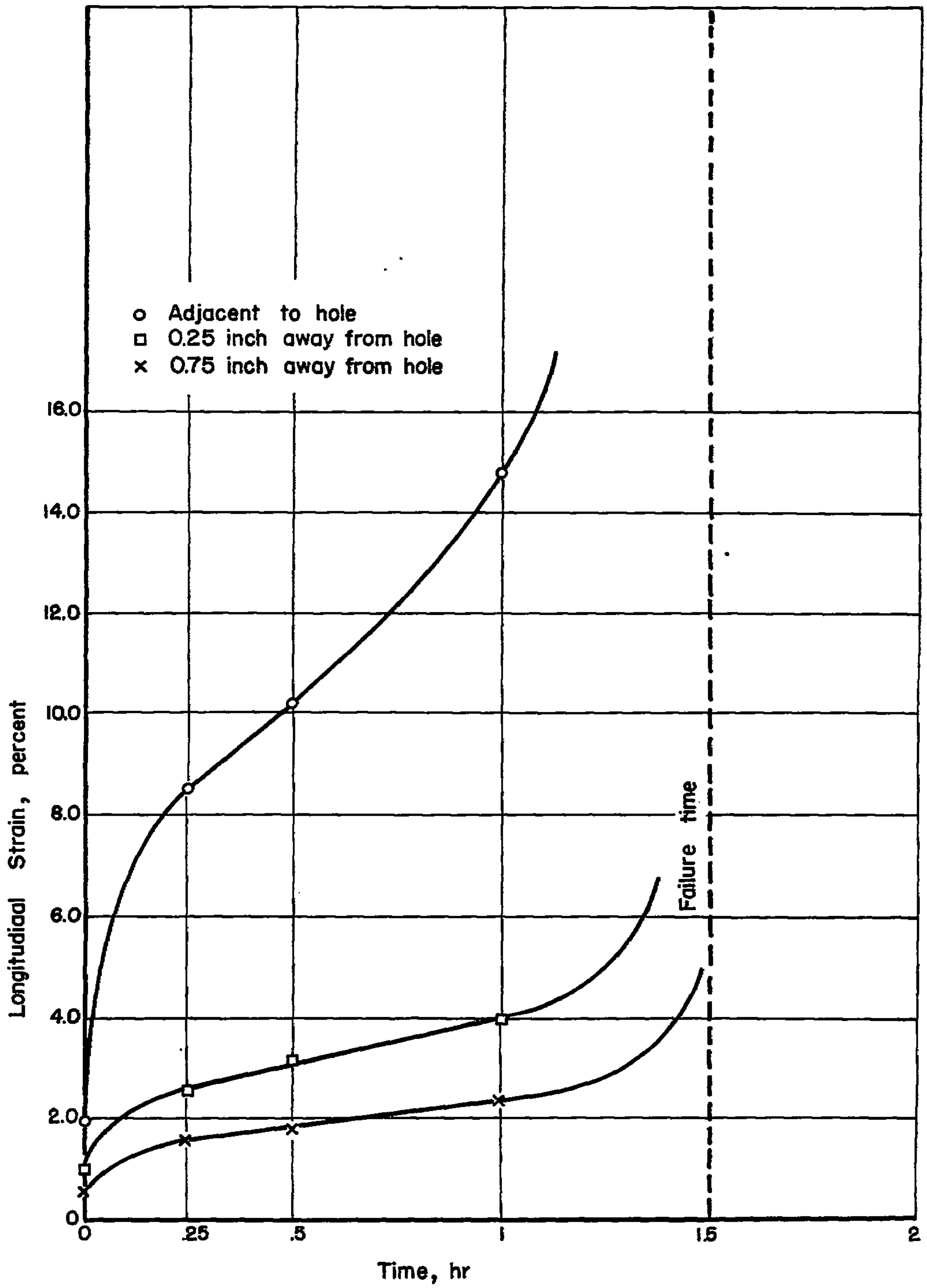

Figure 9.- Strain histories of fibers on line A-A in plate with a hole subjected to tension. Test temperature, 400° F; load, 2,480 pounds; loading ratio P_t/P_b, ∞.

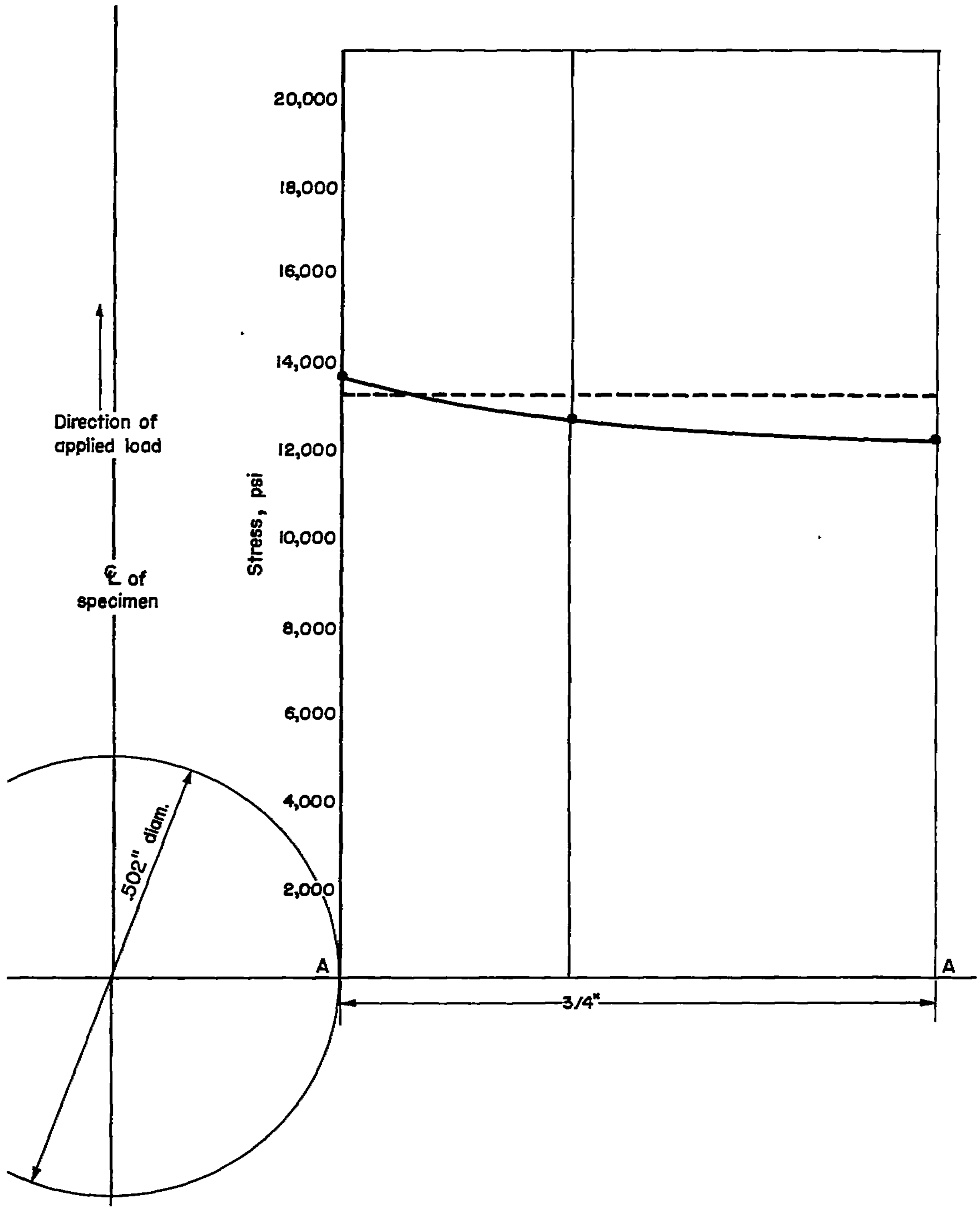

Figure 10.- Stress distribution on line A-A during creep. Broken curve denotes average stress. Test temperature, 400° F; load, 2,480 pounds; loading ratio P_t/P_b, ∞.

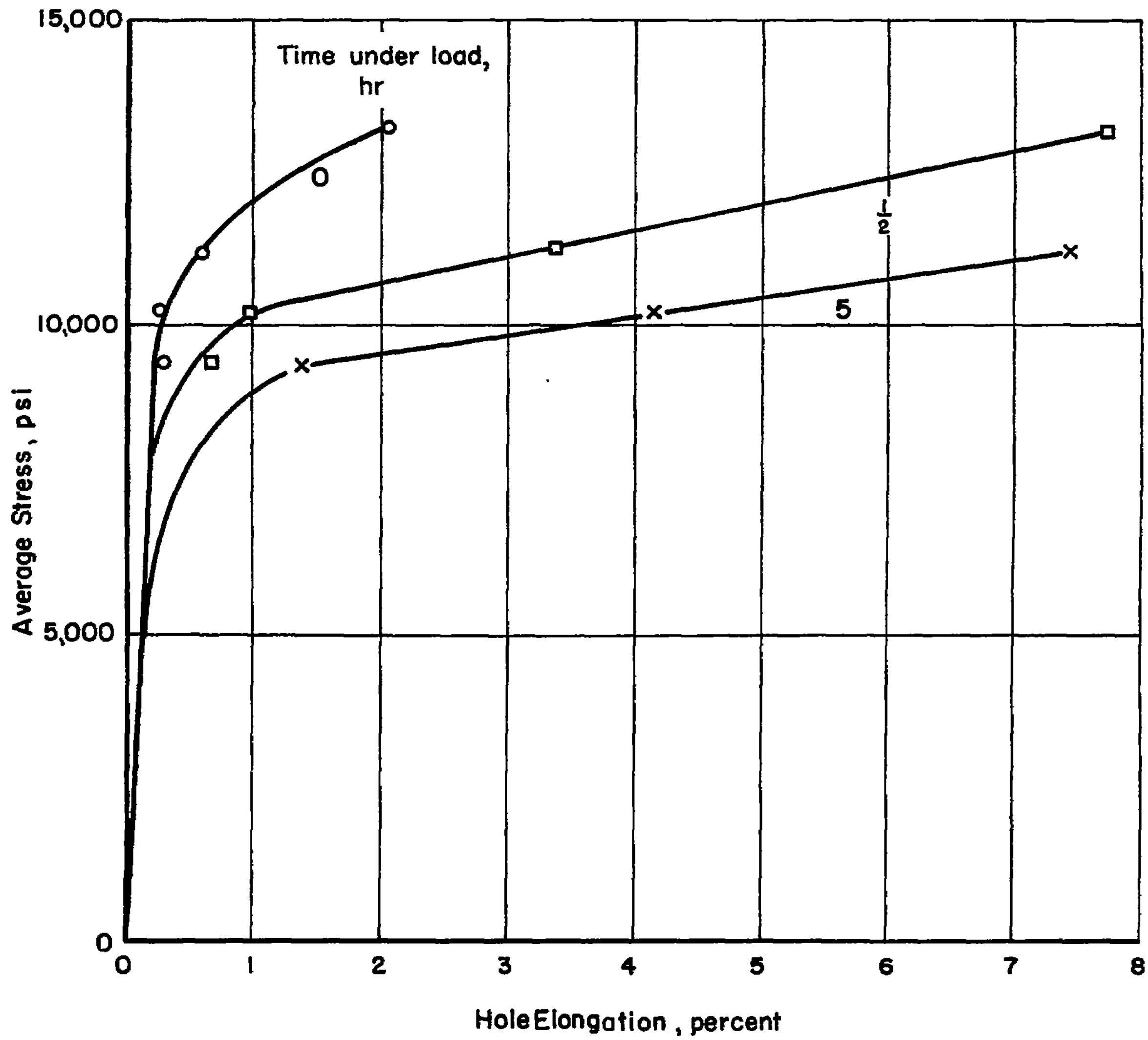

Figure 11.- Elongation of a hole in plate subjected to tension.

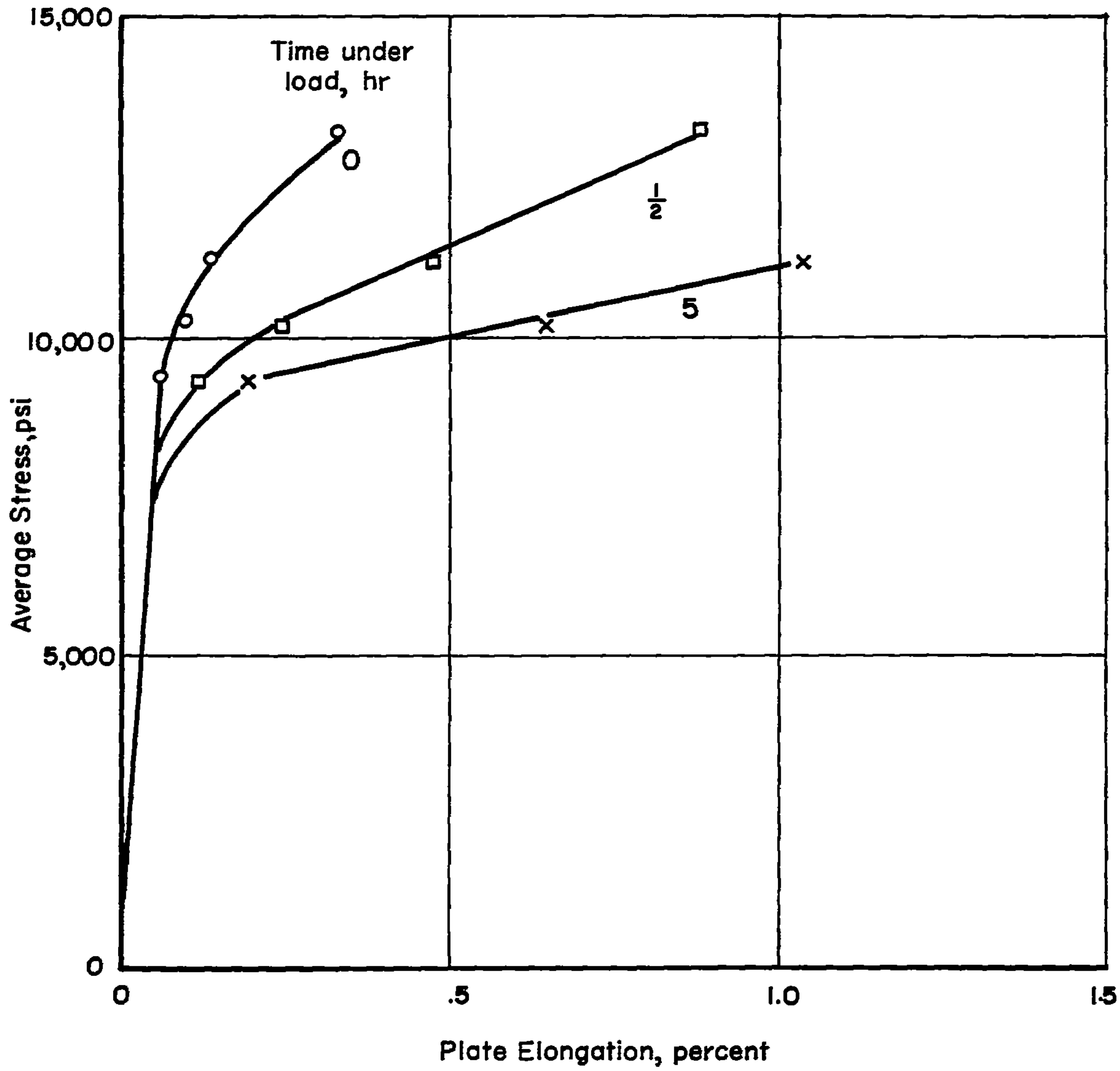

Figure 12.- Elongation in 4 inches of plate with a hole subjected to tension.

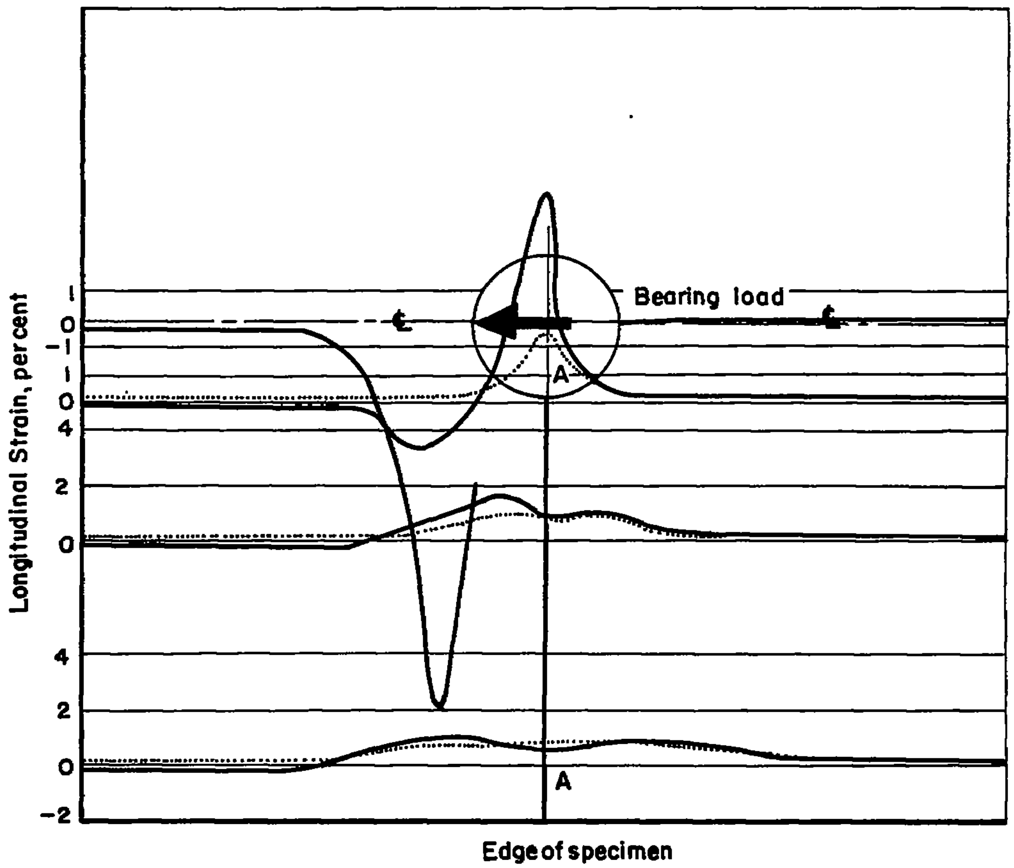

Figure 13.- Typical longitudinal strains on plate with a hole subjected to bearing load. Strains for equivalent tensile load shown by dotted line. Width of specimen has been exaggerated. Loading ratio P_t/P_b, 1; bearing load, 1,720 pounds; time under load, 1/2 hour.

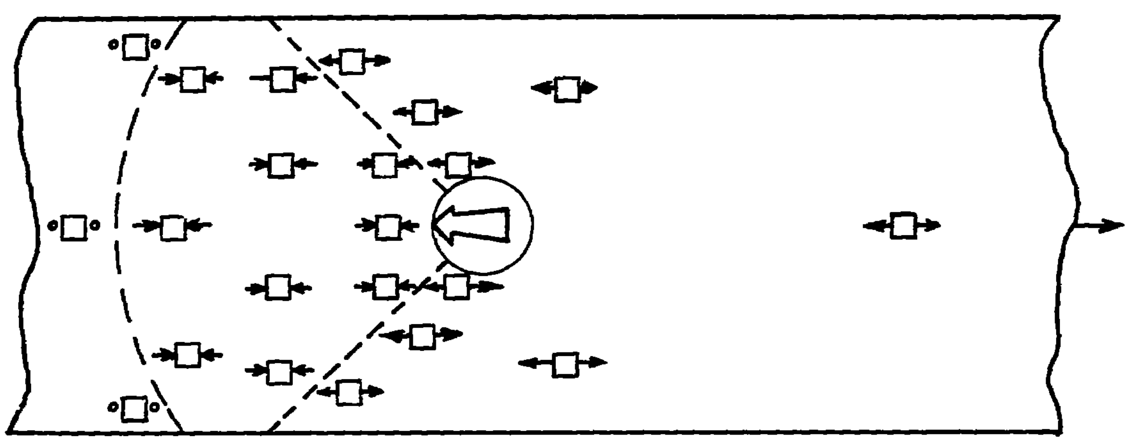

Figure 14.- Area of compression in plate subjected to bearing load.

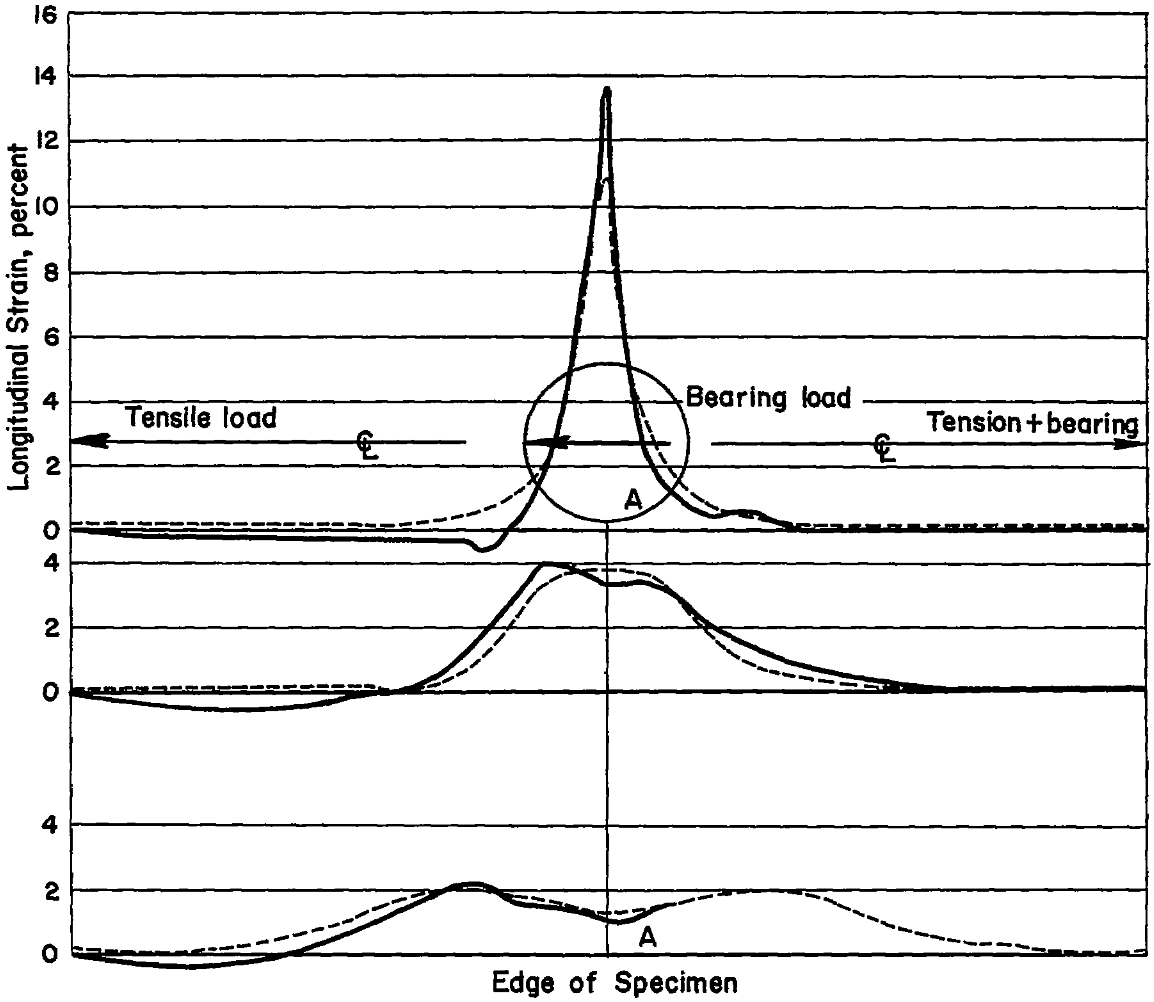

Figure 15.- Typical longitudinal strains on plate with a hole subjected to tension and bearing loads. Strains for equivalent tensile load shown by broken line. Loading ratio $\bar{P}_t/P_b$, 2; tensile load, 960 pounds; bearing load, 960 pounds; time under load, 5 hours.

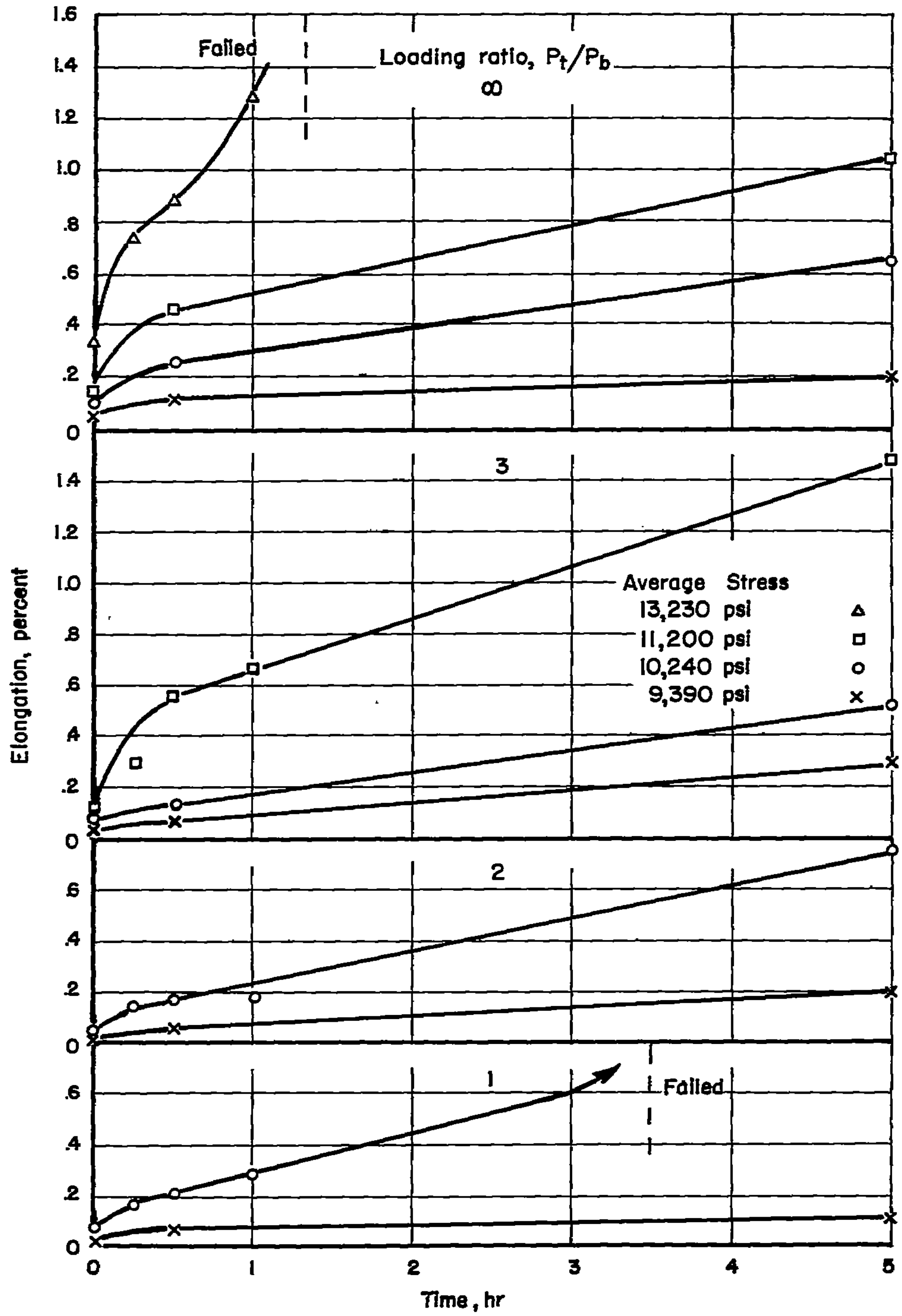

Figure 16.- Elongation in 4 inches of plate with a hole subjected to creep.

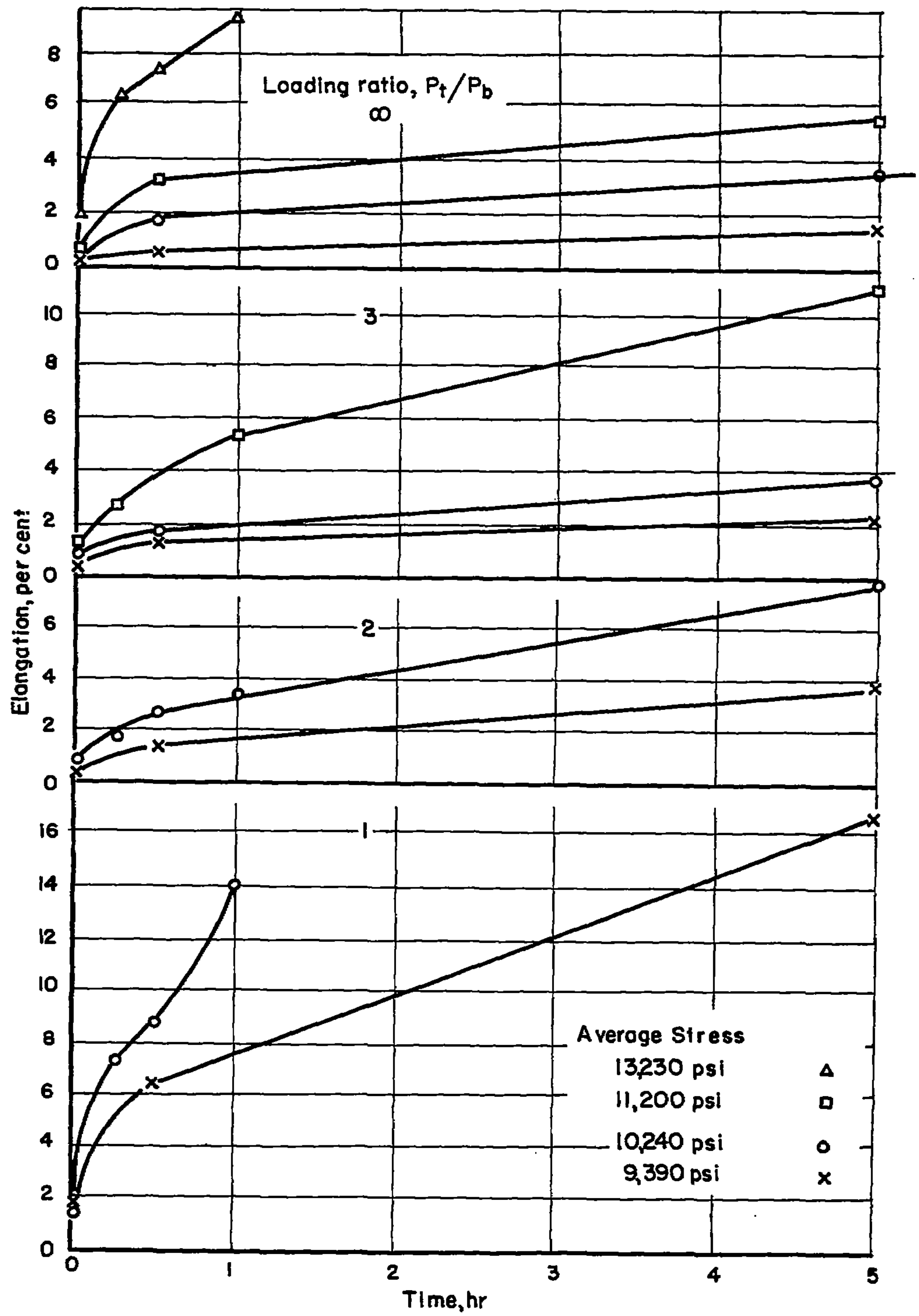

Figure 17.- Elongation of hole in a plate subjected to creep.

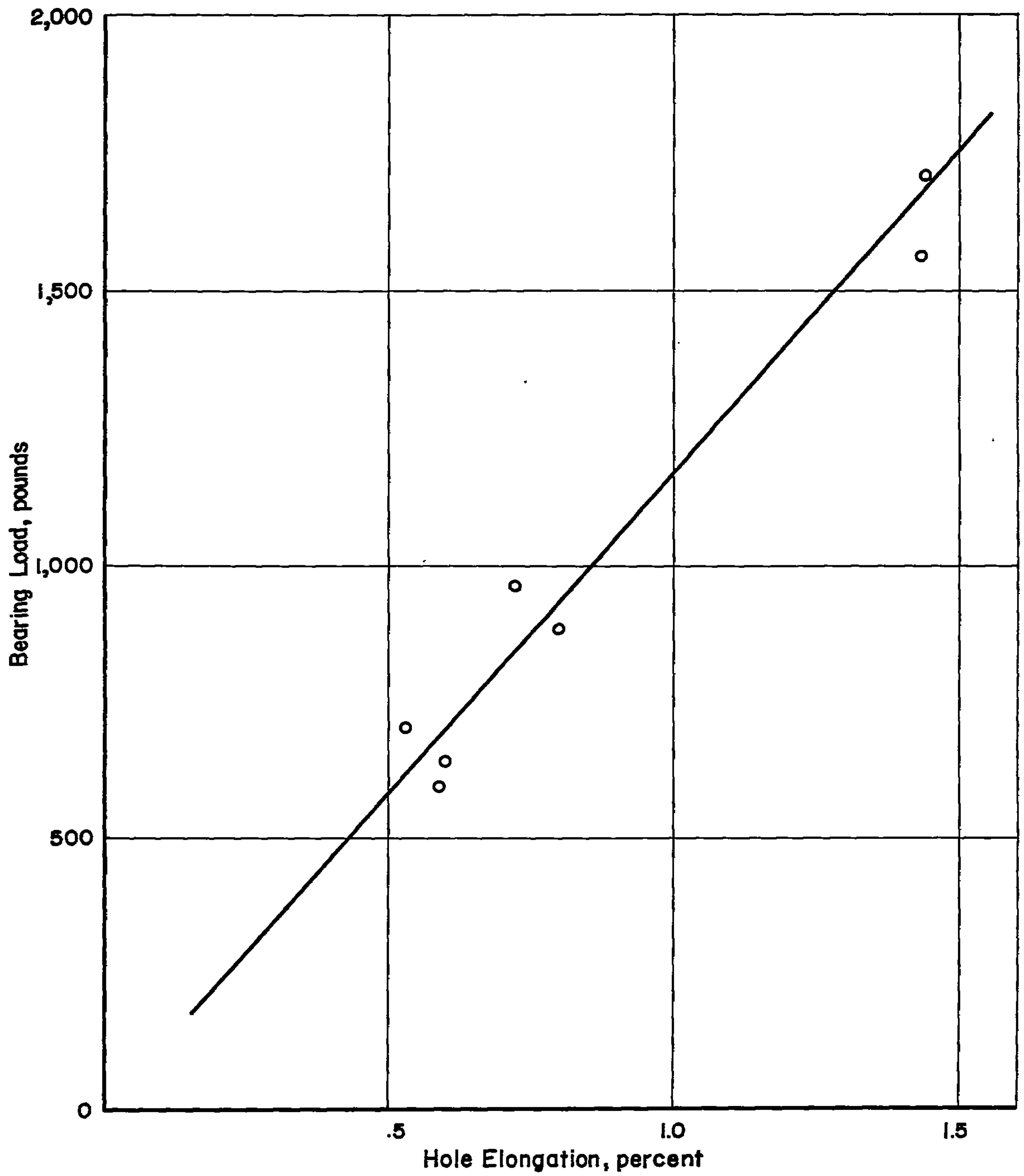

Figure 18.- Hole elongation due to bearing load in plate with a hole.

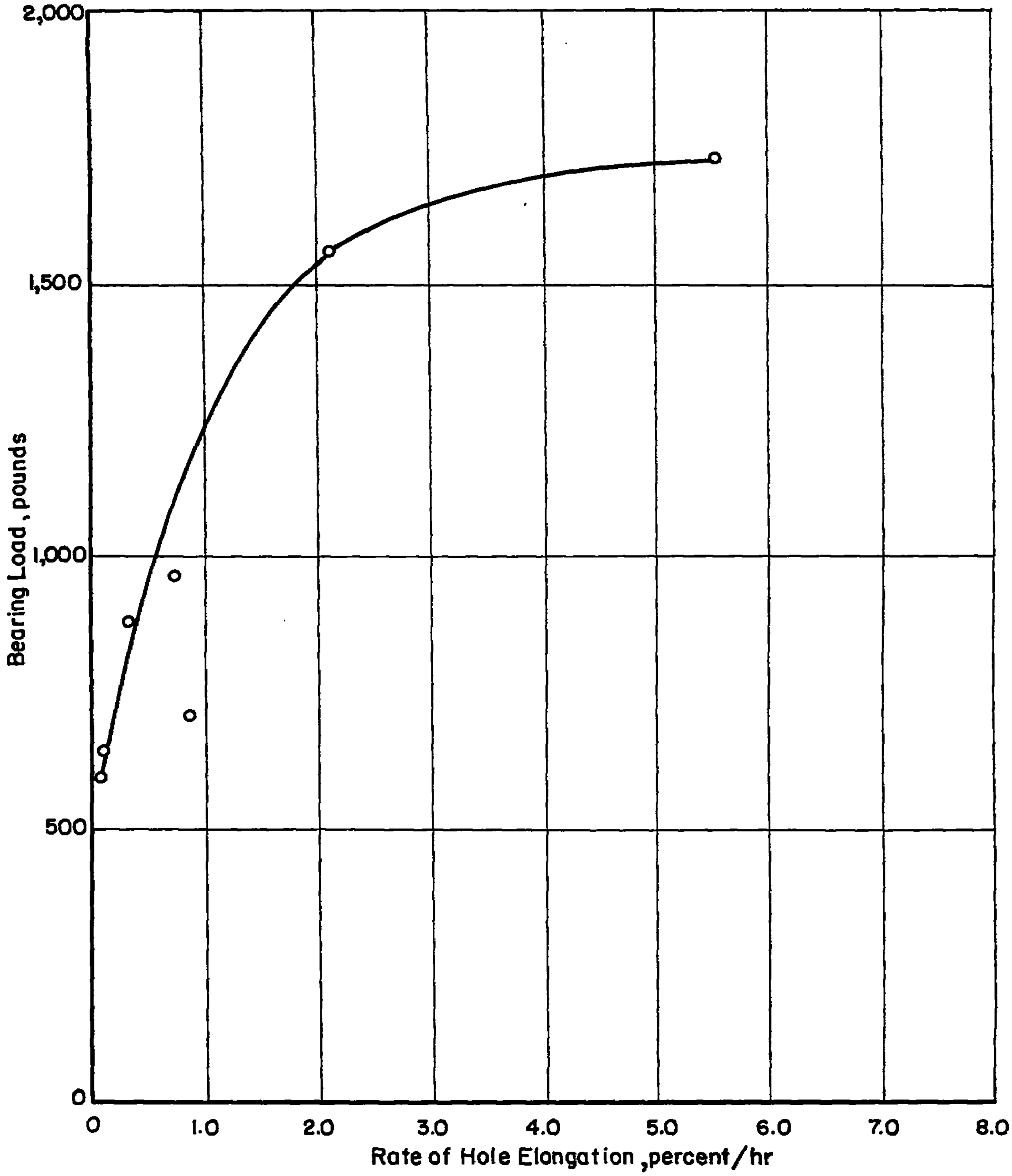

Figure 19.- Effect of bearing load on rate of hole elongation.

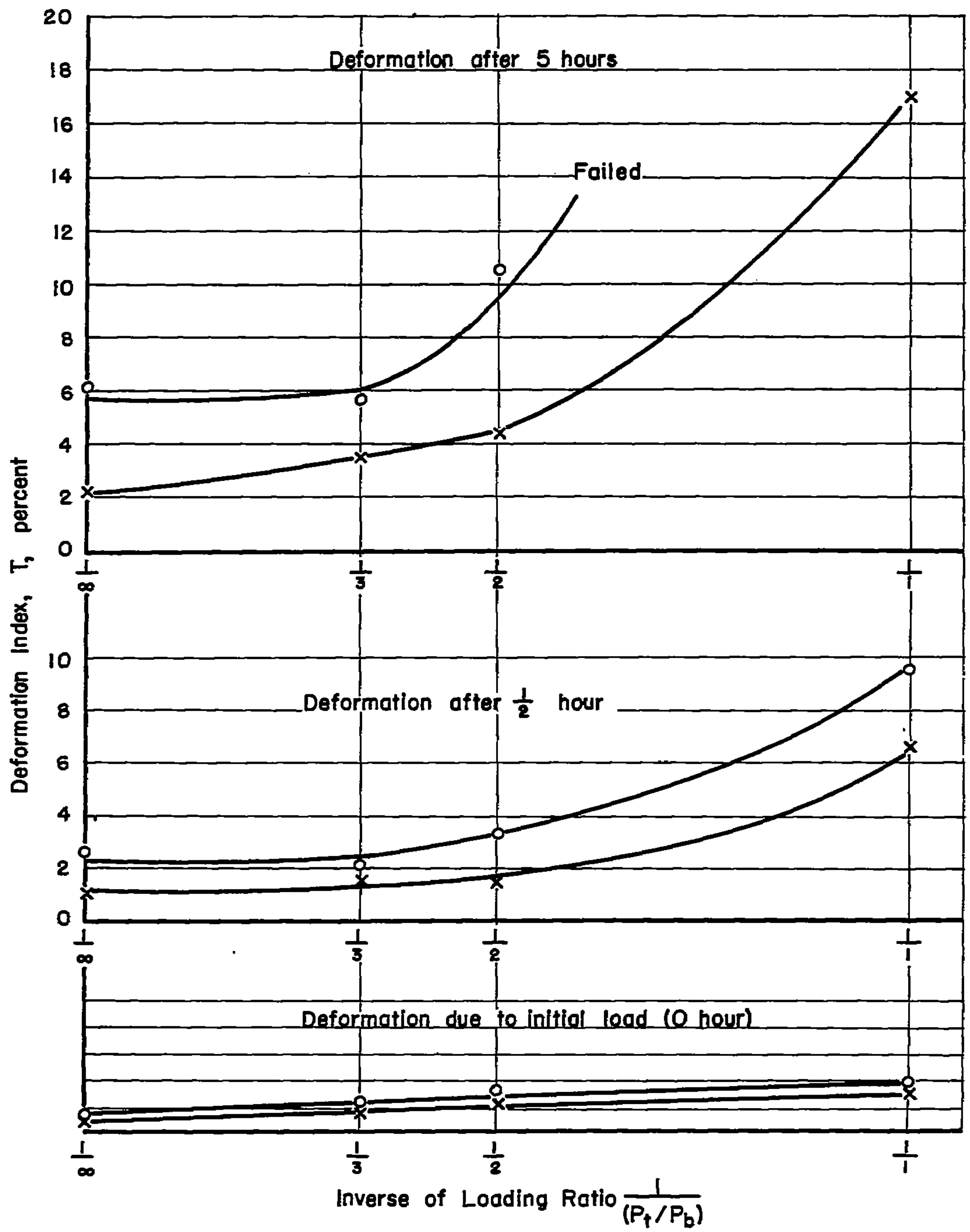

Figure 20.- Effect of loading ratio P_t/P_b on deformation index of riveted joints. Upper curves are for an average stress of 10,240 psi; lower curves are for an average stress of 9,390 psi.

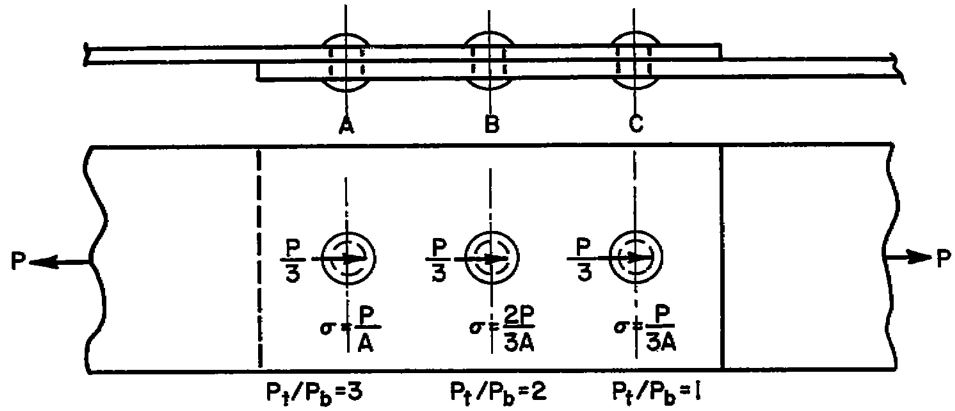

(a) Joint with three rows of rivets.

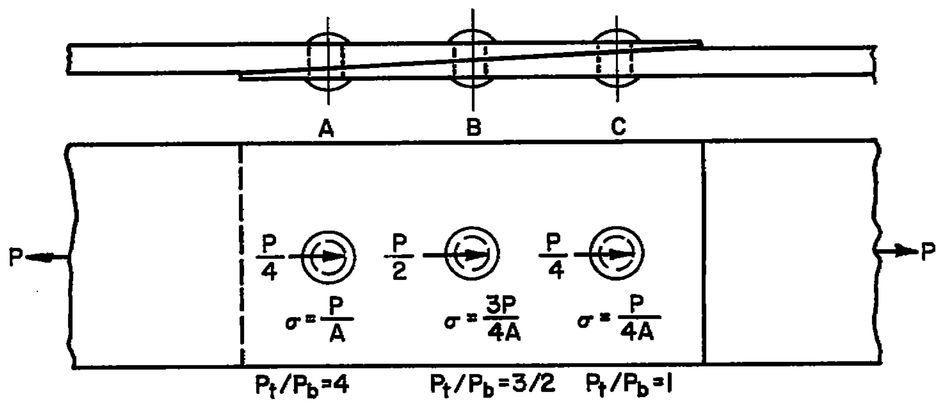

(b) Thickness of plates forming joint has been tapered slightly.

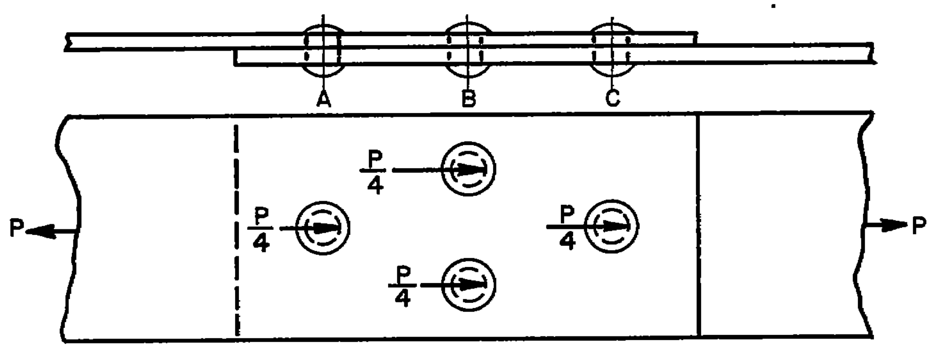

(c) Joint having increased number of rivets along line B.

Figure 21.- Possible designs of simple lap joint. P, load; A, net area across rivet hole, [(Sheet width - Hole diameter) Sheet thickness].